

Ultrafast Electron Transfer Between Dye and Catalyst on a Mesoporous NiO Surface

Allison M. Brown,[§] Liisa J. Antila,[§] Mohammad Mirmohades, Sonja Pullen, Sascha Ott, and Leif Hammarström*

Department of Chemistry - Ångström Laboratory, Uppsala University, Box 523, 75120 Uppsala, Sweden

S Supporting Information

ABSTRACT: The combination of molecular dyes and catalysts with semiconductors into dye-sensitized solar fuel devices (DSSFs) requires control of efficient interfacial and surface charge transfer between the components. The present study reports on the light-induced electron transfer processes of p-type NiO films cosensitized with coumarin C343 and a bioinspired proton reduction catalyst, [FeFe](mcbdt)(CO)₆ (mcbdt = 3-carboxybenzene-1,2-dithiolate). By transient optical spectroscopy we find that ultrafast interfacial electron transfer ($\tau \approx 200$ fs) from NiO to the excited C343 (“hole injection”) is followed by rapid ($t_{1/2} \approx 10$ ps) and efficient surface electron transfer from C343⁻ to the coadsorbed [FeFe](mcbdt)(CO)₆. The reduced catalyst has a clear spectroscopic signature that persists for several tens of microseconds, before charge recombination with NiO holes occurs. The demonstration of rapid surface electron transfer from dye to catalyst on NiO, and the relatively long lifetime of the resulting charge separated state, suggests the possibility to use these systems for photocathodes on DSSFs.

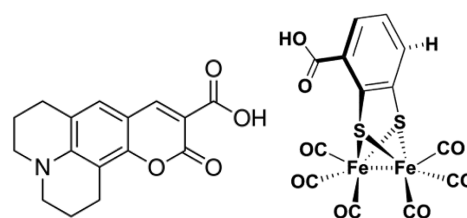
In the quest for solar fuels production, molecular catalysts are promising for efficient splitting of water to form H₂ fuel with O₂ as the clean byproduct.¹ Molecular catalysts allow great tunability of electronic and structural properties via both their first and second coordination sphere. They are amenable to investigations of reaction mechanism and structure/function relationship, allowing for informed design of improved catalysts. The processes of photon absorption, charge separation, and accumulation of redox equivalents all must occur for photo-induced catalysis to transpire. Separation of these tasks relaxes the requirements on any one molecule or component, improving overall effectiveness of catalysis. From research on dye-sensitized solar cells,² we know that photosensitizers are good at absorbing photons and initiating charge separation with a high surface area semiconductor substrate. If a solar fuels catalyst is coupled to this process, photochemical redox accumulation can occur on the molecular catalyst, preparing it for the catalytic process. Thus, a few molecular dye-sensitized solar fuel devices (DSSFs) have been published, with photoanodes for water oxidation or photocathodes for hydrogen production.^{3,4} These electrodes are electronically coupled via an external circuit, either to a dark counter electrode, typically platinum, or in rare cases as a tandem device where both electrodes are photoactive.⁴ For most of these devices, in particular for the photocathodes, there is little

mechanistic information on the processes leading to photo-current and catalysis.

To ensure efficient charge transfer from the dye to the catalyst they can be chemically bound to each other. From a synthetic viewpoint, however, it is much easier to coadsorb dye and catalyst separately on the semiconductor film. This strategy also allows for introducing an antenna function, by using more dyes than catalysts. Coadsorption relies, however, on efficient charge hopping between dye and catalyst on the semiconductor surface. For dye-sensitized TiO₂ it is known that hole hopping between dyes on the surface can occur, and in a few studies, this has been directly demonstrated.⁵ This is promising for the development of photoanodes for water oxidation with molecular dyes and catalysts. For the photocathode side, p-type NiO films are of interest, and a previous study from our group demonstrated that a proton reduction catalyst bound to a NiO film was reduced in <50 ns when a coadsorbed dye was excited.⁶ In the present study, we directly observe the surface electron transfer from reduced dye molecules on NiO to coadsorbed proton reduction catalysts and show that it occurs on an ultrafast time scale. The recombination lifetime of the reduced catalyst with NiO “holes” is very slow in comparison. These results are important for the design of dye-sensitized solar fuel devices based on molecular catalysts, as they suggest that coadsorbed dyes and catalysts can be an efficient way to construct molecular DSSFs.

[FeFe](mcbdt)(CO)₆ (where mcbdt = 3-carboxybenzene-1,2-dithiolate; **Scheme 1**), was chosen as catalyst for this study; the synthesis is described in the **Supporting Information**. The parent complex, [FeFe](bdt)(CO)₆ (bdt = benzene-1,2-dithiolate), is a proton reduction catalyst in solution, inspired by the active site structure of [FeFe]-hydrogenases.⁷ Also the derivatives with the more electron-withdrawing 3,6-dichloro-bdt or 3,6-dicarboxy-bdt ligands are catalytically active in photo-

Scheme 1. Structures of Coumarin 343 and [FeFe](mcbdt)(CO)₆



Received: April 15, 2016

Published: June 17, 2016

catalytic experiments in weakly acidic aqueous media.⁸ Addition of one carboxylic acid group to bdt provides an anchoring group that can tether the complex to a surface, while not being expected to impede catalysis. As dye we chose coumarin 343 (C343, Scheme 1) that is well-known to give ultrafast and efficient hole injection into NiO⁹ and for which the anion is sufficiently reducing to transfer an electron to the catalyst. Mesoporous films of NiO were prepared on fluorine-doped tin oxide or mid-IR transparent CaF₂, using previously described methods.¹⁰ The NiO films were left to soak sequentially in solutions of photosensitizer and catalyst in a dark and inert atmosphere and then rinsed with ethanol prior to experiments; for details see Supporting Information.

Electrochemical reduction of [FeFe](bdt)(CO)₆ in solution occurs as a chemically reversible two-electron process at -1.27 V vs Fc⁺⁰ in CH₃CN due to inverted potentials for the 0/- and -/2- couples.³ For [FeFe](mcbdt)(CO)₆ reduction occurs at E_{1/2} = -1.18 V vs Fc⁺⁰ (Figure S2; Table S1), which ensures a significant driving force for electron transfer from reduced coumarin 343 (E⁰(C343^{0/-}) reported as -1.23 V vs NHE).¹¹ The inverted potentials mean that disproportionation of singly reduced catalysts is energetically feasible. We propose that this may be an advantage in a device, as it may focus reduction equivalents on some catalysts, instead of spreading them on all catalysts on the surface.

Absorbance spectra of the dye and catalyst in solution, as well as of the bare NiO film, were collected prior to sensitization. UV-vis spectra were then collected on the sensitized films to verify the presence of both compounds on the NiO surface. C343 absorbance around 435 nm dominated the spectra, but the presence of [FeFe](mcbdt)(CO)₆ was also clear (Figure S5). Additionally, FTIR spectra of the sensitized films clearly demonstrated the presence of both dye and catalyst on the NiO surface, most obviously by their respective carbonyl bands (Figure S6). The relative band intensities suggest roughly equal surface concentration of the species ([dye]:[catalyst] between 1:2 and 2:1).

The UV-vis absorption spectra of the C343 excited and reduced states were available from previous studies.⁹ For [FeFe](mcbdt)(CO)₆ only the absorbance spectra for the ground and doubly reduced species were attainable through spectroelectrochemistry because of the inverted potentials. Instead, the spectrum of the reduced [FeFe](mcbdt)(CO)₆⁻ species was determined by transient absorption after a laser flash-quench cycle with [Ru(bpy)₃]²⁺ and a donor.¹² This ensures single reduction of the catalyst on a submicrosecond time scale by the flash generated [Ru(bpy)₃]⁺; see SI for details. From the transient absorption signals the [FeFe](mcbdt)(CO)₆⁻ spectrum could be determined (Figure 1) by subtraction of the spectrum of the oxidized donor. The spectra obtained from independent experiments with TTF (tetrathiafulvalene) and TMPD (*N,N,N',N'*-tetramethyl-phenylene-1,4-diamine) as donors were in good agreement (Figure 1). The neutral catalyst has a relatively weak absorption in the visible region. Single reduction will give a band around 480 nm, while two-electron reduction will give a band around 580 nm, very similar to what was determined for [FeFe](bdt)(CO)₆.¹² These features can be used to determine the oxidation state of the catalyst in transient absorption experiments.

Spectra on the subpicosecond to nanosecond time scale following laser pulse excitation (435 nm, 120 fs pulses) were collected to follow the photoinduced electron transfer processes after excitation of C343 coadsorbed with [FeFe](mcbdt)(CO)₆

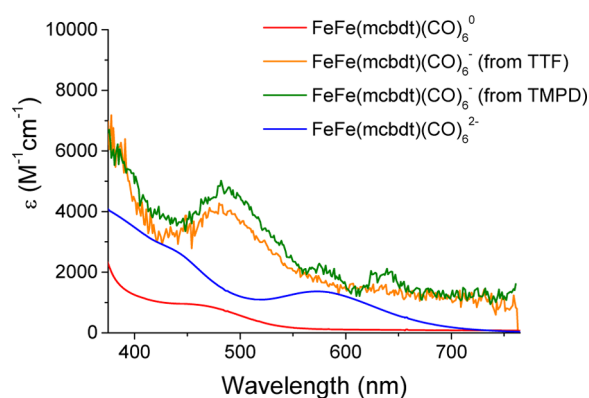


Figure 1. Absorption spectra of [FeFe](mcbdt)(CO)₆ (red) and [FeFe](mcbdt)(CO)₆²⁻ generated by electrolysis (blue), and of [FeFe](mcbdt)(CO)₆⁻ as determined from laser flash-quench experiments with [Ru(bpy)₃]²⁺ and TTF (orange) or TMPD (green) as electron donors (see text). All spectra were collected in 2:1 MeCN/MeOH.

on the surface of mesoporous NiO films (samples denoted FeFe/C343|NiO). Excitation of C343 on NiO without catalyst (C343|NiO) has been well studied previously,⁹ and the agreement of the present study is good. We also found that initial behavior (*t* < 1 ps) is the same when [FeFe](mcbdt)(CO)₆ is coadsorbed with C343 (Figure 2, Figure S7). Upon excitation of C343|NiO or

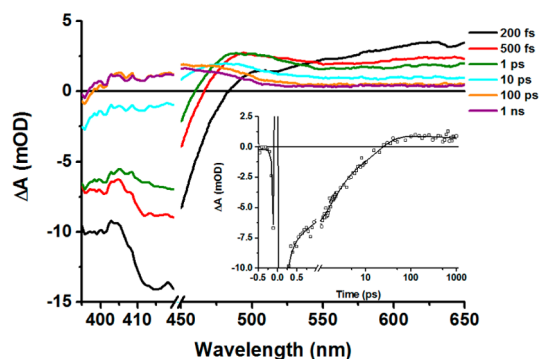


Figure 2. Transient absorption spectra of the FeFe/C343|NiO sample from 200 fs to 1 ns after excitation with 430 nm, ~120 fs pulses. The inset shows the time evolution of the transient absorption at 410 nm, which predominantly monitors the reoxidation of C343⁻ (bleach recovery) and the concomitant reduction of [FeFe(mcbdt)(CO)₆]⁻ (induced absorption).

FeFe/C343|NiO, a strong negative signal containing ground state bleach (GSB) and stimulated emission (SE) is immediately seen from 400 to 500 nm as well as a weak, broad absorbance red of 550 nm. The SE decays on a ca. 200 fs time scale, but the GSB remains and the positive feature blue-shifts, resulting in a net absorption from 460 nm and above. This is consistent with ultrafast hole injection from excited C343 and formation of the C343⁻ anion.⁹ Apparently, this behavior is not significantly perturbed by coadsorption of [FeFe](mcbdt)(CO)₆. However, in the C343|NiO sample the C343⁻/NiO⁽⁺⁾ state remains for tens to hundreds of picoseconds before recombination to the ground state.⁹ In contrast, the FeFe/C343|NiO sample shows a very rapid disappearance of the C343⁻ anion features with a half-life *t*_{1/2} ≈ 10 ps. The absorption at >550 nm decreases, and the ground state bleach at 390–450 nm recovers to be replaced by an absorption band with a maximum around 460 nm (Figure 2).

The absorption recovery/rise at 410 nm and the decay at 600 nm follow very similar, nonexponential kinetics (Figure S8). A fit to the data using a sum of three exponents (τ_1 – τ_3) and a residual long-lived component (τ_4) gave the lifetimes reported in Table 1.

Table 1. Lifetimes from a Four Exponential Fit to the fs–ps Data for FeFe|C343|NiO

λ probe (nm)	τ_1 (A ₁)	τ_2 (A ₂)	τ_3 (A ₃)	τ_4 (A ₄)
410	<200 fs (-67%)	1.7 ps (-19%)	17 ps (-11%)	>1 ns (3%)
600	250 fs (36%)	1.4 ps (32%)	36 ps (20%)	>1 ns (12%)

The 460 nm absorption persists for the duration of the experiment, longer than 1 ns, and is followed on the ns– μ s time scale in separate experiments described in the next section. The spectrum most closely resembles that of the singly reduced catalyst [FeFe](mcbdt)(CO)₆⁻ (Figure 1), although slightly blue-shifted (*vide infra*). Control experiments on a sample without C343 (FeFe|NiO) showed comparatively small and featureless signals that decayed predominantly on a time scale of 200 fs (Figure S9). Thus, we can attribute the positive absorption around 460 nm formed with $t_{1/2} \approx 10$ ps in FeFe|C343|NiO to the reduced catalyst, formed by hole injection from the excited C343 and subsequent surface electron transfer from C343⁻ to the catalyst.

Nanosecond transient absorption after a 10 ns laser flash at 470 nm was used to follow the long-lived species observed in the fs experiments. The earliest recorded spectrum (120 ns) shows maxima centered around 480 and 710 nm, as well as to the blue of 400 nm (Figure 3). The <400 and 480 nm peaks correspond well

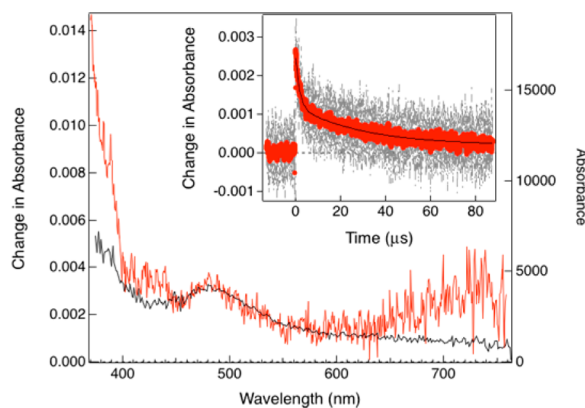


Figure 3. Transient absorption spectrum of the FeFe|C343|NiO sample at 120 ns after 10 ns laser excitation at 470 nm (red); absorption spectrum of reduced [FeFe](mcbdt)(CO)₆⁻ from Figure 1 (black). Inset: kinetic trace at 480 nm, with a biexponential fit ($\tau_1 = 2 \mu\text{s}$ and $\tau_2 = 30 \mu\text{s}$); gray points are raw data, red points are binned data, and black line is the fit.

to the singly reduced catalyst [FeFe](mcbdt)(CO)₆⁻ in solution (Figure 1). The agreement with solution data shows that the slight blue-shift of the visible band that was seen in the ultrafast experiments (at 460 nm) is not just because the complex is attached to NiO. One tentative explanation is instead that the structural changes known to occur upon reduction (twisting of the bdt and breaking of one Fe–S bond)¹² may take longer than 1 ns.

The signals of [FeFe](mcbdt)(CO)₆⁻ decay on a μ s time scale; a biexponential fit gave $\tau_1 = 2 \mu\text{s}$ and $\tau_2 = 30 \mu\text{s}$ with similar amplitudes. Thus, recombination of the reduced catalyst with NiO holes occurs on a very slow time scale compared to the fs–ps reactions of initial light induced charge separation. We did not observe any formation of doubly reduced catalyst on the time scale of the experiment. Disproportionation of reduced catalysts on the NiO surface is apparently slower than charge recombination.

We directly observe electron transfer from dyes to catalysts cosensitized on the surface of mesoporous films of p-type NiO, with $t_{1/2} \approx 10$ ps. This is at least 3 orders of magnitude faster than what is reported for the analogous process of “hole” hopping between molecular dyes on mesoporous TiO₂.⁵ This is a surprisingly large difference. One contributing factor could be the significant driving force for electron transfer to the catalyst in the present case, while the systems on TiO₂ have often involved self-exchange between identical dyes ($\Delta G^0 = 0$); this is probably only part of the explanation, however. It seems likely that most of the excited C343 dyes are in close proximity to a catalyst molecule so that direct, short-distance electron transfer can occur. This suggests that the dyes and catalyst jointly approach monolayer coverage or that they preferentially bind in close proximity even at submonolayer coverage.

The broad signal centered around 710 nm is not present in solution phase [FeFe](mcbdt)(CO)₆ in either oxidation state, does not resemble NiO holes in spectroelectrochemical experiments,¹³ and is not seen in the C343|NiO experiments. It decays, however, with the same kinetics as the band at 480 nm (Figure S10). This signal is, therefore, assigned to the charge transfer state. It could be a charge transition between the reduced, [FeFe](mcbdt)(CO)₆⁻ and NiO. Alternatively, the NiO holes generated by transient charge separation on a μ s time scale may have different spectral properties from those generated by electrolysis on a time scale of minutes.

It is also important that we see no evidence for any fraction of unreactive C343⁻. This shows that there are no isolated dyes or segregated islands of dyes on the NiO surface that are not in close contact with catalysts. Alternatively, if there are islands, electron hopping between dyes to reach a catalyst nonetheless occurs on the 10 ps time scale. In any case, the rapid and complete electron transfer from the photogenerated C343⁻ dyes competes favorably with the dye–NiO recombination and results in a high efficiency of photoinduced catalyst reduction. The yield of electron transfer to the catalyst can be roughly estimated to 40–80%, from the C343⁻ signal after 1 ps ($\epsilon_{590} = 4200 \text{ M}^{-1} \text{ cm}^{-1}$)¹⁵ and the [FeFe]⁻ signal at 100 ps ($\epsilon_{480} = 4000 \text{ M}^{-1} \text{ cm}^{-1}$; Figure 1) in Figure 2 (see SI for details). The loss of yield can be attributed to C343⁻–NiO⁽⁺⁾ recombination that occurs on a similar time scale as electron transfer to the catalyst.

The comparatively slow recombination of FeFe|C343|NiO⁽⁺⁾ is rewarding. It is interesting to note that all investigated dye/NiO systems have so far shown recombination on the ps time scale, and suppression of recombination out to the μ s time scale has only been reported for dye-acceptor dyads,¹⁴ or with a coadsorbed acceptor.⁶ We see no reason to assume a weaker electronic coupling of [FeFe](mcbdt)(CO)₆ to NiO, via the aromatic mcbdt ligand, than for the dyes in question. We are currently investigating the origin of this favorable result. In any case, the relatively long-lived charge separation suggests that further steps of catalysis, i.e., transfer of protons and a second electron, may have time to occur. This result may pave the way

for the design of H₂-producing photocathodes based on molecularly cosensitized p-type semiconductors.

■ ASSOCIATED CONTENT

5 Supporting Information

The Supporting Information is available free of charge on the ACS Publications website at DOI: 10.1021/jacs.6b03889.

Synthesis and characterization of [FeFe](mcbdt)(CO)₆, experimental procedures, transient absorption data, and electron transfer yield calculations (PDF)

■ AUTHOR INFORMATION

Corresponding Author

*leif.hammarstrom@kemi.uu.se.

Author Contributions

[§]These authors contributed equally to the work.

Notes

The authors declare no competing financial interest.

■ ACKNOWLEDGMENTS

Financial support from The Knut and Alice Wallenberg Foundation, The Swedish Energy Agency, and The Carl Trygger Foundation is gratefully acknowledged.

■ REFERENCES

- (1) (a) Hammarström, L. *Acc. Chem. Res.* **2015**, *48*, 840. (b) Berardi, S.; Drouet, S.; Francàs, L.; Gimbert-Suriñach, C.; Guttentag, M.; Richmond, C.; Stolla, T.; Llobet, A. *Chem. Soc. Rev.* **2014**, *43*, 7501. (c) Eckenhoff, W. T.; Eisenberg, R. *Dalton Trans.* **2012**, *41*, 13004.
- (2) (a) Yella, A.; Lee, H.-W.; Tsao, H. N.; Yi, C. Y.; Chandiran, A. K.; Nazeeruddin, M. K.; Diau, E. W.-G.; Yeh, C.-Y.; Zakeeruddin, S. M.; Graetzel, M. *Science* **2011**, *334*, 629. (b) Hagfeldt, A.; Boschloo, G.; Sun, L.; Kloo, L.; Pettersson, H. *Chem. Rev.* **2010**, *110*, 6595.
- (3) (a) Ashford, D. L.; Gish, M. K.; Vannucci, A. K.; Brennaman, M. K.; Templeton, J. L.; Papanikolas, J. M.; Meyer, T. J. *Chem. Rev.* **2015**, *115*, 13006. (b) Queyriaux, N.; Kaeffer, N.; Morozan, A.; Chavarot-Kerlidou, M.; Artero, V. *J. Photochem. Photobiol., C* **2015**, *25*, 90. (c) Bachmeier, A.; Hall, S.; Ragsdale, S. W.; Armstrong, F. A. *J. Am. Chem. Soc.* **2014**, *136*, 13518. (d) Ji, Z.; He, M.; Huang, Z.; Ozkan, U.; Wu, Y. *J. Am. Chem. Soc.* **2013**, *135*, 11696. (e) Moore, G. F.; Blakemore, J. D.; Milot, R. L.; Hull, J. F.; Song, H.-E.; Cai, L.; Schmuttenmaer, C. A.; Crabtree, R. H.; Brudvig, G. W. *Energy Environ. Sci.* **2011**, *4*, 2389. (f) Li, L.; Duan, L.; Xu, Y.; Gorlov, M.; Hagfeldt, A.; Sun, L. *Chem. Commun.* **2010**, *46*, 7307.
- (4) (a) Li, F.; Fan, K.; Xu, B.; Gabrielsson, E.; Daniel, Q.; Li, L.; Sun, L. *J. Am. Chem. Soc.* **2015**, *137*, 9153. (b) Fan, K.; Li, F.; Wang, L.; Daniel, Q.; Gabrielsson, E.; Sun, L. *Phys. Chem. Chem. Phys.* **2014**, *16*, 25234.
- (5) (a) Hu, K.; Robson, K. C. D.; Beauvilliers, E. E.; Schott, E.; Zarate, X.; Arratia-Perez, R.; Berlinguette, C. P.; Meyer, G. J. *J. Am. Chem. Soc.* **2014**, *136*, 1034. (b) Brennan, B. J.; Durrell, A. C.; Koepf, M.; Crabtree, R. H.; Brudvig, G. W. *Phys. Chem. Chem. Phys.* **2015**, *17*, 12728. (c) Ardo, S.; Meyer, G. J. *J. Am. Chem. Soc.* **2010**, *132*, 9283.
- (6) Gardner, J. M.; Beyler, M.; Karnahl, M.; Tschierlei, S.; Ott, S.; Hammarström, L. *J. Am. Chem. Soc.* **2012**, *134*, 19322.
- (7) (a) Capon, J. F.; Gloaguen, F.; Schollhammer, P.; Talarmin, J. *J. Electroanal. Chem.* **2006**, *595*, 47. (b) Felton, G. A. N.; Vannucci, A. K.; Chen, J.; Lockett, L. T.; Okumura, N.; Petro, B. J.; Zakai, U. I.; Evans, D. H.; Glass, R. S.; Lichtenberger, D. L. *J. Am. Chem. Soc.* **2007**, *129*, 12521.
- (8) (a) Pullen, S.; Fei, H.; Orthaber, A.; Cohen, S.; Ott, S. *J. Am. Chem. Soc.* **2013**, *135*, 16997. (b) Streich, D.; Astuti, Y.; Orlandi, M.; Schwartz, L.; Lomoth, R.; Hammarström, L.; Ott, S. *Chem. - Eur. J.* **2010**, *16*, 60.
- (9) (a) Morandeira, A.; Boschloo, G.; Hagfeldt, A.; Hammarström, L. *J. Phys. Chem. C* **2008**, *112*, 9530. (b) Morandeira, A.; Boschloo, G.; Hagfeldt, A.; Hammarström, L. *J. Phys. Chem. B* **2005**, *109*, 19403.
- (10) Li, L.; Gibson, E. A.; Qin, P.; Boschloo, G.; Gorlov, M.; Hagfeldt, A.; Sun, L. *Adv. Mater.* **2010**, *22*, 1759.

(11) (a) Hara, K.; Sato, T.; Katoh, R.; Furube, A.; Ohga, Y.; Shinpo, A.; Suga, S.; Sayama, K.; Sugihara, H.; Arakawa, H. *J. Phys. Chem. B* **2003**, *107*, 597. (b) Nominally, this would correspond to ca. -1.61 V vs. Fc⁺⁰, but the exact value has to be taken with caution because of the junction potential between the DMF solution and the Ag/AgCl (KCl sat.) reference electrode used.

(12) Mirmohades, M.; Pullen, S.; Stein, M.; Maji, S.; Ott, S.; Hammarström, L.; Lomoth, R. *J. Am. Chem. Soc.* **2014**, *136*, 17366.

(13) Boschloo, G.; Hagfeldt, A. *J. Phys. Chem. B* **2001**, *105*, 3039.

(14) Odobel, F.; Pellegrin, Y.; Gibson, E. A.; Hagfeldt, A.; Smeigh, A. L.; Hammarström, L. *Coord. Chem. Rev.* **2012**, *256*, 2414. (b) Morandeira, A.; Fortage, J.; Edvinsson, T.; Le Pleux, L.; Blart, E.; Boschloo, G.; Hagfeldt, A.; Hammarström, L.; Odobel, F. *J. Phys. Chem. C* **2008**, *112*, 1721. (c) Daeneke, T.; Yu, Z.; Lee, G. P.; Fu, D.; Duffy, N. W.; Makuta, S.; Tachibana, Y.; Spiccia, L.; Mishra, A.; Bäuerle, P.; Bach, U. *Adv. Energy Mater.* **2015**, *5*, 1401387.

(15) Nad, S.; Pal, H. *J. Phys. Chem. A* **2002**, *106*, 6823.